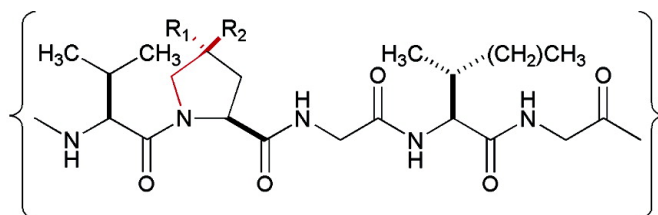


A Stereoelectronic Effect on Turn Formation Due to Proline Substitution in Elastin-Mimetic Polypeptides

Wookhyun Kim, R. Andrew McMillan, James P. Snyder, and Vincent P. Conticello

J. Am. Chem. Soc., **2005**, 127 (51), 18121-18132 • DOI: 10.1021/ja054105j • Publication Date (Web): 02 December 2005

Downloaded from <http://pubs.acs.org> on March 25, 2009



Elastin-1: $R_1 = H$, $R_2 = H$; Elastin-2: $R_1 = H$, $R_2 = F$; Elastin-3: $R_1 = F$, $R_2 = H$

More About This Article

Additional resources and features associated with this article are available within the HTML version:

- Supporting Information
- Links to the 6 articles that cite this article, as of the time of this article download
- Access to high resolution figures
- Links to articles and content related to this article
- Copyright permission to reproduce figures and/or text from this article

[View the Full Text HTML](#)

A Stereoelectronic Effect on Turn Formation Due to Proline Substitution in Elastin-Mimetic Polypeptides

Wookhyun Kim,[†] R. Andrew McMillan,^{‡,§} James P. Snyder,[†] and Vincent P. Conticello^{*,†}

Contribution from the Department of Chemistry, Emory University, 1515 Dickey Drive, Atlanta, Georgia 30322, and Bioengineering Branch, NASA Ames Research Center, Moffett Field, California 94035

Received June 21, 2005; E-mail: vcontic@emory.edu

Abstract: Stereoelectronic effects have been identified as contributing factors to the conformational stability of collagen-mimetic peptide sequences. To assess the relevance of these factors within other protein structural contexts, three polypeptide sequences were prepared in which the sequences were derived from the canonical repeat unit (Val-Pro-Gly-Val-Gly) of the protein material elastin. These elastin-mimetic polypeptides, **elastin-1**, **elastin-2**, and **elastin-3**, incorporate (2*S*)-proline, (2*S*,4*S*)-4-fluoroproline, and (2*S*,4*R*)-4-fluoroproline, respectively, at the second position of the elastin repeat. Calorimetric and spectroscopic investigations of these three polypeptides indicate that the incorporation of the substituted proline residues had a dramatic effect upon the self-assembly of the corresponding elastin peptide. The presence of (2*S*,4*R*)-4-fluoroproline in **elastin-3** lowered the temperature of the phase transition and increased the type II β -turn population with respect to the parent polypeptide, while the presence of (2*S*,4*S*)-4-fluoroproline in **elastin-2** had the opposite effect. These results suggest that stereoelectronic effects could either enhance or hinder the self-assembly of elastin-mimetic polypeptides, depending on the influence of the proline analogue on the energetics of the β -turn conformation that develops within the pentapeptide structural repeats above the phase transition. Density functional theory (DFT) was employed to model three possible turn types (β_1 -, β_{II} -, and inverse γ -turns) derived from model peptide segments (MeCO-Xaa-Gly-NHMe) (Xaa = Pro, 4*S*-F-Pro, or 4*R*-F-Pro) corresponding to the turn-forming residues of the elastin repeat unit (Val-Pro-Gly-Val-Gly). The results of these calculations suggested a similar outcome to the experimental data for the elastin-mimetic polypeptides, in that type II β -turn structures were stabilized for peptide segments containing (2*S*,4*R*)-fluoroproline and destabilized for segments containing (2*S*,4*S*)-fluoroproline relative to the canonical proline residue.

Introduction

Stereoelectronic effects have been identified recently as contributing factors to the conformational stability of proteins, the influence of which can be particularly dramatic within specific structural contexts.¹ For example, structural investigations of collagen-mimetic peptides have demonstrated that the thermodynamics of self-assembly of the native triple helical structure can be modulated by stereoelectronic effects that arise from introduction of electronegative substituents onto the proline ring.^{2–6} In particular, the thermodynamic stability of the triple helix can be interpreted in terms of the effect of the electro-

negative substituent on the conformation of the pyrrolidine ring as it influences the local secondary structure of the collagen peptide. These studies have provided insight into the role of post-translational hydroxylation of proline residues in stabilizing the triple helical structure of native collagens,⁷ as well as a rationale for the design of non-native collagen analogues with enhanced stabilities for biomedical applications. We present results herein that suggest that stereoelectronic effects are not limited to collagen-mimetic peptide sequences and may be employed as a more general method for modifying the conformational dynamics of proline residues in native protein sequences with structural implications for protein design and

[†] Emory University.

[‡] NASA Ames Research Center.

[§] Current address: 5AM Ventures, 3000 Sand Hill Road, Menlo Park, CA 94025.

- (1) DeRider, M. L.; Wilkens, S. J.; Waddell, M. J.; Bretscher, L. E.; Weinhold, F.; Raines, R. T.; Markley, J. L. *J. Am. Chem. Soc.* **2002**, *124*, 2497–2505.
- (2) (a) Hodges, J. A.; Raines, R. T. *J. Am. Chem. Soc.* **2003**, *125*, 9262–9263. (b) Bretscher, L. E.; Jenkins, C. L.; Taylor, K. M.; DeRider, M. L.; Raines, R. T. *J. Am. Chem. Soc.* **2001**, *123*, 777–778. (c) Holmgren, S. K.; Bretscher, L. E.; Taylor, K. M.; Raines, R. T. *Chem. Biol.* **1999**, *6*, 63–70. (d) Holmgren, S. K.; Taylor, K. M.; Bretscher, L. E.; Raines, R. T. *Nature* **1998**, *392*, 666–667.

- (3) (a) Barth, D.; Milbradt, A. G.; Renner, C.; Moroder, L. *ChemBioChem* **2004**, *5*, 79–86. (b) Barth, D.; Musiol, H. M.; Schutt, M.; Fiori, S.; Milbradt, A. G.; Renner, C.; Moroder, L. *Chemistry* **2003**, *9*, 3692–702.
- (4) Persikov, A. V.; Ramshaw, J. A.; Kirkpatrick, A.; Brodsky, B. *J. Am. Chem. Soc.* **2003**, *125*, 11500–11501.
- (5) Doi, M.; Nishi, Y.; Uchiyama, S.; Nishiuchi, Y.; Nakazawa, T.; Ohkubo, T.; Kobayashi, Y. *J. Am. Chem. Soc.* **2003**, *125*, 9922–3.
- (6) (a) Umashankara, M.; Babu, I. R.; Ganesh, K. N. *Chem. Commun.* **2003**, 2606–2607. (b) Babu, I. R.; Ganesh, K. N. *J. Am. Chem. Soc.* **2001**, *123*, 2079–2080.
- (7) Berg, R. A.; Prockop, D. J. *Biochem. Biophys. Res. Commun.* **1973**, *52*, 115–120.

engineering.⁸ We provide evidence that elastin-mimetic polypeptide sequences are susceptible to stereoelectronic effects that alter the thermodynamics of self-assembly of the protein and suggest that this phenomenon can be rationalized in terms of the influence of proline substitution on the energetics of the β -turn conformations that develop within the pentapeptide structural repeats above the phase transition.

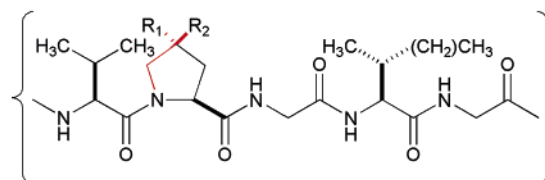
The proteinaceous material elastin is the primary structural component underlying the elastomeric mechanical response of compliant tissues in vertebrates⁹ and is, therefore, of considerable interest as a biocompatible material for tissue engineering applications.¹⁰ Native elastin is derived from post-translational processing of the precursor protein, tropoelastin, which consists of a modular sequence of alternating, structurally distinct elastomeric and cross-linkable domains. The elastomeric domains comprise structurally similar oligopeptide motifs that are tandemly repeated in the native protein sequence. The local secondary structure and macromolecular thermodynamic and viscoelastic properties of the elastomeric domains can be emulated by synthetic polypeptides that are composed of a concatenated sequence of the native oligopeptide motifs, the most common of which is the pentapeptide [Val-Pro-Gly-Val-Gly].¹¹ Polypeptides based on these pentameric repeat sequences undergo reversible, temperature-dependent, hydrophobic assembly from aqueous solution in analogy to the phase behavior of native tropoelastin. This process results in spontaneous phase separation of the polypeptide above a lower critical solution temperature, T_l , which coincides with a conformational rearrangement of the local secondary structure within the pentapeptide motifs. Biophysical studies of elastin and elastin-mimetic polypeptides have indicated an essential role for the proline residues with regard to structure development within the pentapeptide repeats.^{12–17} In particular, proline residues within the repeats participate in the formation of type II β -turn structural units, which increase in population within the [Val-Pro-Gly-Val-Gly] repeats as the temperature approaches the phase transition of the polypeptide. The facility with which this process occurs critically influences the thermodynamics of the phase transition and is crucial for assembly of the physiologically relevant coacervate state of native elastin. However, conventional protein structural determination methods (i.e., multi-dimensional solution NMR and X-ray diffraction analysis) are of limited use for structural analysis of the condensed elastin-rich phases that arise above the transition temperature, which hinders our ability to evaluate the structural importance of the proline residues with respect to elastin assembly.

In analogy with structural investigations of proline substitution in collagen-mimetic peptides,^{2–6} the incorporation of structurally

Scheme 1^a

A. **Elastin-1**: MGH₁₀S₂GHID₄KHM [(VPGVG)₄VPGIG]₁₆V

B.



Elastin-1: $R_1 = H, R_2 = H$; **Elastin-2**: $R_1 = H, R_2 = F$; **Elastin-3**: $R_1 = F, R_2 = H$

^a (A) Complete amino acid sequence of the elastin-mimetic polypeptide, **elastin-1**. (B) Structural formulas of the pentapeptide repeat units corresponding to the elastomeric domains of **elastin-1**, **elastin-2**, and **elastin-3**. The bond vectors that define the stereoelectronic fluorine-amide gauche interactions within the pyrrolidine ring of the proline residue are highlighted in color.

modified proline analogues with altered stereoelectronic properties into the pentapeptide repeats of elastin-mimetic polypeptides may provide insight into the relationship between the local structural parameters that define the β -turn conformation and the macromolecular thermodynamics of elastin assembly. We recently reported biosynthetic methods for the cotranslational incorporation of a structurally diverse series of proline analogues into the elastin-mimetic polypeptide **elastin-1**,¹⁸ which afforded the elastin analogues **elastin-2** and **elastin-3**, in which the canonical proline residues were substituted with (2*S*,4*S*)-4-fluoroproline and (2*S*,4*R*)-4-fluoroproline, respectively (Scheme 1). These polypeptides were envisioned as potentially useful substrates to assess the role of stereoelectronic effects due to proline substitution on elastin assembly. Stereoelectronic interactions between vicinal CF and NH bonds separated by two carbons (i.e., FC–CC–NH) strongly influence the conformational energetics of piperidines¹⁹ and have been proposed to have the same effect in pyrrolidine rings. Of particular relevance to the peptide-based systems under consideration in this study, stereoelectronic gauche interactions between vicinal fluorine and amide substituents²⁰ have been demonstrated to strongly influence the conformational energetics of the pyrrolidine ring of substituted proline derivatives in small-molecule model compounds.^{1,8,21–23} The (4*S*)- and (4*R*)-fluoroproline epimers preferentially adopt alternative conformations of the pyrrolidine ring corresponding to the *C γ* -endo pucker and the *C γ* -exo pucker, respectively. Structural investigations of fluoroproline substitution on collagen-mimetic peptides have established that the pyrrolidine ring conformation exerts an influence on the conformational thermodynamics of a polypeptide chain through

- (8) Renner, C.; Alefelder, S.; Bae, J. H.; Budisa, N.; Huber, R.; Moroder, L. *Angew. Chem., Int. Ed.* **2001**, *40*, 923–925.
 (9) Rosenbloom, J.; Abrams, W. R.; Mecham, R. *FASEB J.* **1993**, *7*, 1208–1218.
 (10) Langer, R.; Tirrell, D. A. *Nature* **2004**, *428*, 487–492.
 (11) Urry, D. W. In *Protein-Based Materials*; McGrath, K. P., Kaplan, D., Eds.; Birkhauser: Boston, 1997; pp 133–177.
 (12) Urry, D. W.; Shaw, R. G.; Prasad, K. U. *Biochem. Biophys. Res. Commun.* **1985**, *130*, 50–57.
 (13) Thomas, G. J., Jr.; Prescott, B.; Urry, D. W. *Biopolymers* **1987**, *36*, 921–934.
 (14) Urry, D. W.; Krishna, N. R.; Huang, D. H.; Trapane, T. L.; Prasad, K. U. *Biopolymers* **1989**, *28*, 819–833.
 (15) Reiersen, H.; Clarke, A. R.; Rees, A. R. *J. Mol. Biol.* **1998**, *283*, 255–264.
 (16) Li, B.; Alonso, D. O.; Daggett, V. *J. Mol. Biol.* **2001**, *305*, 581–592.
 (17) Yao, X. L.; Hong, M. *J. Am. Chem. Soc.* **2004**, *126*, 4199–4210.

- (18) Kim, W.; George, A.; Evans, M. E.; Conticello, V. P. *ChemBioChem* **2004**, *5*, 928–936.
 (19) (a) Lankin, D. C.; Chandrakumar, N. S.; Rao, S. N.; Spangler, D. P.; Snyder, J. P. *J. Am. Chem. Soc.* **1993**, *115*, 3356–3357. (b) Snyder, J. P.; Chandrakumar, N. S.; Sato, H.; Lankin, D. C. *J. Am. Chem. Soc.* **2000**, *122*, 544–545. (c) Lankin, D. C.; Grunewald, G. L.; Romero, F. A.; Oren, I. Y.; Snyder, J. P. *Org. Lett.* **2002**, *4*, 3557–3560. (d) Sun, A.; Lankin, D. C.; Hardcastle, K.; Snyder, J. P. *Chem.–Eur. J.* **2005**, *11*, 1579–1591.
 (20) (a) O'Hagan, D.; Bilton, C.; Howard, J. A. K.; Knight, L.; Tozer, D. J. *J. Chem. Soc., Perkin Trans. 2* **2000**, 605–607. (b) Briggs, C. R. S.; O'Hagan, D.; Howard, J. A. K.; Yufit, D. S. *J. Fluorine Chem.* **2003**, *119*, 9–13.
 (21) (a) Eberhardt, E. S.; Panasiak, N., Jr.; Raines, R. T. *J. Am. Chem. Soc.* **1996**, *118*, 12261–12266. (b) Panasiak, N., Jr.; Eberhardt, E. S.; Edison, A. S.; Powell, D. R.; Raines, R. T. *Int. J. Pept. Protein Res.* **1994**, *44*, 262–269.
 (22) (a) Improta, R.; Benzi, C.; Barone, V. *J. Am. Chem. Soc.* **2001**, *123*, 12568–12577. (b) Improta, R.; Mele, F.; Crescenzi, O.; Benzi, C.; Barone, V. *J. Am. Chem. Soc.* **2002**, *124*, 7857–7865. (c) Benzi, C.; Improta, R.; Scalmani, G.; Barone, V. *J. Comput. Chem.* **2002**, *23*, 341–350.
 (23) Mooney, S. D.; Kollman, P. A.; Klein, T. E. *Biopolymers* **2002**, *64*, 63–71.

its effect on the local dihedral angles (ϕ , ψ , ω) associated with the substituted proline residues.^{1–5}

We hypothesized that elastin-mimetic polypeptides might also be susceptible to stereoelectronic effects that manifest themselves through their influence on the local conformation within the pentapeptide repeats. The most suggestive evidence in support of this hypothesis arises from consideration of the crystal structure of a cyclic trimer of the elastin repeat sequence, *cyclo*-(Val-Pro-Gly-Val-Gly)₃.²⁴ The individual pentapeptide units within this structure adopt a type II β -turn conformation in which the pyrrolidine rings of the proline residues at the ($i + 1$) positions of the turn uniformly display a *C γ -exo* ring pucker. In contrast, a conformational analysis of native proteins and polypeptides within the structural database indicated that *trans*-proline residues within turn conformations do not display a significant preference between pyrrolidine ring puckers.²⁵ These apparently conflicting observations raise the question of whether the *C γ -exo* ring pucker of the proline residues within the cyclic trimer may be a persistent feature associated with the pentapeptide repeats in elastin-mimetic sequences and native elastin, potentially implying a determinative role for proline conformation in the formation of the type II β -turn structures associated with elastin assembly. In consideration of this hypothesis, we anticipated that incorporation of the 4-fluoroproline epimers into the pentapeptide repeats of the elastin-mimetic polypeptide sequence **elastin-1** might introduce a stereochemical bias with respect to the development of the type II β -turn conformation among the pentapeptide units during the elastin assembly. The distinct conformational preferences of (4*S*)- versus (4*R*)-fluoroproline would suggest an alternative destabilization or stabilization of the *C γ -exo* ring pucker, respectively. Thus the substitution of these noncanonical proline residues into the elastin-mimetic polypeptides **elastin-2** and **elastin-3** could influence the development of the β -turn structure within the pentapeptide repeats potentially altering the elastin phase transition. This investigation would provide structural insight into the importance of the proline ring conformation on the thermodynamics of the phase transition, which can have significant implications for the *de novo* design of elastin-based biomaterials for applications in tissue engineering^{26–29} and biotechnology.^{30–32}

Results and Discussion

Biosynthesis of Elastin Analogues. Elastin-mimetic polypeptides **elastin-1**, **elastin-2**, and **elastin-3** (Scheme 1) were prepared as previously described using the *E. coli* auxotrophic host strain DG99 (*proC*::Tn10) upon expression of the target gene from a modified pQE-80 plasmid in the presence of the

respective proline derivative.¹⁸ A similar protocol was employed to produce variants of **elastin-1**, **-2**, and **-3** in which the nitrogen atoms of the nonproline residues within the respective polypeptides were uniformly labeled with the ¹⁵N isotope for ¹H–¹⁵N HSQC NMR spectroscopic experiments. The target proteins were purified to homogeneity from the endogenous proteins of the bacterial host as fusions to a *N*-terminal decahistidine sequence using immobilized metal affinity chromatography. The decahistidine leader sequence was retained in the elastin derivatives employed in subsequent calorimetric and spectroscopic analyses. Due to its small size relative to the repetitive elastin sequence, it was anticipated that the leader sequence would not significantly influence the physical properties of the macromolecules and was shown to behave accordingly. The isolated yields of the polypeptides were approximately 45–50 mg/L for fully induced expression cultures in modified minimal medium (NMM) under conventional batch fermentation conditions in shake flask culture. The protein yields of **elastin-2** and **elastin-3** were comparable to the parent sequence **elastin-1** and are quite respectable, especially in consideration of the high analogue content within the respective polypeptide sequences. Amino acid compositional analysis and MALDI-TOF mass spectrometry of the elastin derivatives indicated virtually complete substitution of proline with the respective imino acid analogue as previously described.¹⁸ Little residual proline content was detected in the recombinant target proteins, and the molecular ions within the mass spectra corresponded well with the calculated masses for elastin derivatives in which the encoded proline residues were completely substituted with the respective proline analogues. The ¹⁹F NMR analyses of **elastin-2** and **elastin-3** demonstrated spectroscopic features that were commensurate with high levels of incorporation of the respective fluoroproline derivative in comparison to the canonical amino acid within the same structural context.¹⁸

Calorimetric Measurement of the Elastin Phase Transition. Differential scanning calorimetry (DSC) provides a convenient method for determination of the thermodynamic parameters associated with the elastin assembly from aqueous solution.³³ DSC measurements on dilute aqueous solutions (ca. 1.0 mg/mL) of the elastin-mimetic polypeptides **elastin-1**, **-2**, and **-3** indicated that the value of the transition temperature, T_t , associated with the endothermic transition depended dramatically on the identity of the proline analogue that had been incorporated into the polypeptide sequence (Figure 1). The (4*S*)- and (4*R*)-fluoroproline-substituted elastins displayed transition temperatures that were shifted toward higher (41.1 °C) and lower (21.6 °C) temperatures, respectively, in comparison with the T_t of the parent polypeptide, **elastin-1** (33.1 °C). In support of the observed trend in T_t , the van't Hoff enthalpies calculated from the DSC data decrease in the order: **elastin-3** (+908 ± 16 kJ mol⁻¹) > **elastin-1** (+879 ± 9 kJ mol⁻¹) > **elastin-2** (+782 ± 13 kJ mol⁻¹).³⁴ These results are in agreement with previously observed endothermic transition enthalpies (ΔH) for elastin-mimetic polymers¹¹ and block-copolymers³⁵ and indicate an entropy-driven (positive ΔS) process consistent with hydropho-

(24) Cook, W. J.; Einspahr, H.; Trapane, T. L.; Urry, D. W.; Bugg, C. E. *J. Am. Chem. Soc.* **1980**, *102*, 5502–5505.

(25) Milner-White, E. J.; Lachlan, H. B.; Maccallum, P. H. *J. Mol. Biol.* **1992**, *228*, 725–734.

(26) Urry, D. W. *Trends Biotechnol.* **1999**, *17*, 249–257.

(27) Welsh, E. R.; Tirrell, D. A. *Biomacromolecules* **2000**, *1*, 23–30.

(28) Keeley, F. W.; Bellingham, C. M.; Woodhouse, K. A. *Philos. Trans. R. Soc. London, Ser. B* **2002**, *357*, 185–189.

(29) Mithieux, S. M.; Rasko, J. E.; Weiss, A. S. *Biomaterials* **2004**, *25*, 4921–4927.

(30) Wright, E. R.; Conticello, V. P. *Adv. Drug Delivery Rev.* **2002**, *54*, 1057–1073.

(31) Chilkoti, A.; Dreher, M. R.; Meyer, D. E. *Adv. Drug Delivery Rev.* **2002**, *54*, 1093–1111.

(32) (a) Meyer, D. E.; Chilkoti, A. *Nat. Biotechnol.* **1999**, *17*, 1112–1115. (b) Ge, X.; Yang, D. S.; Trabbic-Carlson, K.; Kim, B.; Chilkoti, A.; Filipe, C. D. *J. Am. Chem. Soc.* **2005**, *127*, 11228–11229. (c) Banki, M. R.; Feng, L.; Wood, D. W. *Nat. Methods* **2005**, *2*, 659–662.

(33) Luan, C.-H.; Harris, R. D.; Prasad, K. U.; Urry, D. W. *Biopolymers* **1990**, *29*, 1699–1706.

(34) Calculated ΔH per mol of pentamer: **elastin-1**, 11.0 ± 0.11 kJ mol⁻¹; **elastin-2**, 9.78 ± 0.16 kJ mol⁻¹; **elastin-3**, 11.4 ± 0.20 kJ mol⁻¹.

(35) (a) Wright, E. R.; McMillan, R. A.; Cooper, A.; Apkarian, R. P.; Conticello, V. P. *Adv. Funct. Mater.* **2002**, *2*, 149–154. (b) Lee, T. A. T.; Cooper, A.; Apkarian, R. P.; Conticello, V. P. *Adv. Mat.* **2000**, *12*, 1105–1110.

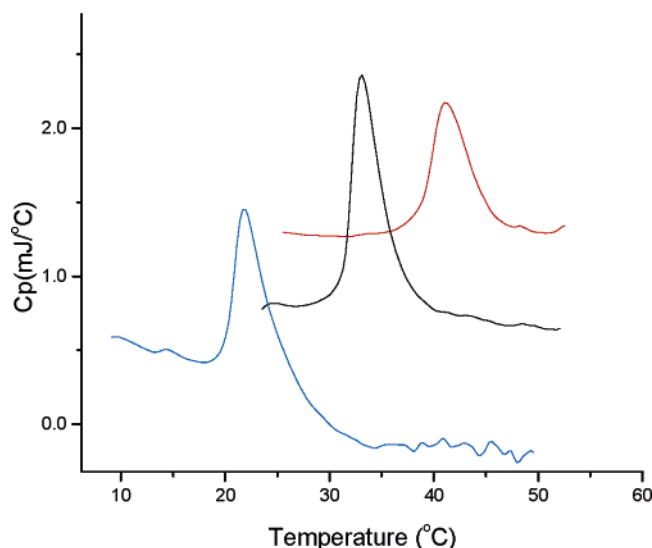


Figure 1. Raw differential scanning calorimetry data for dilute aqueous solutions (1.0 mg/mL) of **elastin-1** (black), **elastin-2** (red), and **elastin-3** (blue). Note the pronounced decrease in baseline for **elastin-3** after the calorimetric transition, which corresponds to the observed heat capacity decrement (negative ΔC_p) associated with the endothermic process.

bic or other solvation-related interactions. These calorimetric data imply that the entropic driving force associated with the hydrophobic assembly process is greatest for **elastin-3**. Significantly in this regard, **elastin-3** is the only polypeptide that, at low concentration (≤ 1.0 mg/mL), displays a measurable decrease in apparent heat capacity ($\Delta C_p = -24.5 \pm 0.92$ kJ mol $^{-1}$ K $^{-1}$ or -0.66 J K $^{-1}$ g $^{-1}$) above the transition temperature (as indicated by the change in baseline for **elastin-3** in Figure 1). This heat capacity decrement is usually indicative of the formation of noncovalent interactions associated with a hydrophobic assembly process. The value of ΔC_p for **elastin-3** compares well to the average values seen upon folding of globular proteins from the denatured state to a more compact native fold (mean $\Delta C_p \approx -0.48 \pm 0.14$ J K $^{-1}$ g $^{-1}$ at 25 °C),^{36,37} which suggests that the aggregation of polypeptide chains observed for **elastin-3** resembles, at least in part, the burial of peptide groups in a compact protein fold.

We suggest that the differences in thermodynamic parameters observed between **elastin-2** and **elastin-3**, particularly vis-à-vis the parent polypeptide **elastin-1**, may be attributed to the influence of stereoelectronic effects due to the presence of the substituted proline residues on the energetics of elastin assembly. Previous calorimetric and turbidimetric studies of the self-assembly of elastin analogues demonstrated that large differences could be observed in the transition temperature of elastin-mimetic polypeptides due to amino acid substitutions in the pentapeptide repeat sequence.^{38,39} The structurally noncritical fourth position of the elastin repeat sequence is tolerant of nonconservative substitutions such that variant polypeptides can be synthesized in which guest residues replace the canonical Val⁴ residue within the pentapeptides at differing levels of fractional incorporation. These amino acid substitutions alter

the position of the phase transition of the elastin analogues in a manner that depends strongly on the polarity of the amino acid side chain of the guest residues and the mole fraction of the variant pentapeptides within the elastin sequence. The observed differences in thermodynamic parameters of the variant elastin polypeptide sequence with respect to the consensus sequence have been rationalized in terms of the effect of the amino acid substitutions on the hydration shell of the elastin polypeptides rather than intrinsic structural effects. However, we believe that this phenomenon cannot account for the significant difference in transition temperature observed between **elastin-2** and **elastin-3**, which are identical in composition, sequence, and molar mass and are distinguished only with respect to the configuration of the asymmetric center at C-4 on the structurally critical proline derivative.

Conformational Analysis of Elastin Polypeptides. If indeed stereoelectronic effects give rise to the observed differences in the thermodynamics of assembly among the elastin derivatives, these intrinsic structural effects should become apparent through their influence on the polypeptide conformation. Circular dichroism (CD) spectroscopy was employed to examine the implications of this hypothesis, particularly in the context of secondary structure development within the pentapeptide repeats during the thermal transition in dilute aqueous solution. Prior CD studies of elastin-mimetic polypeptides indicated that a conformational rearrangement occurred as the temperature increased through the transition point, which corresponded to a conversion of the local secondary structure of the pentapeptide repeats from a random coil conformation to a more ordered type II β -turn conformation.^{12,15} This conformational transition can be detected in the CD spectra of **elastin-1** as a function of temperature in that the random coil signature (negative ellipticity near 195 nm) is gradually replaced with the type II β -turn signature (positive ellipticity near 207 nm) as the temperature is increased through the transition point (Figure 2).^{12,15,40} Similar behavior is observed in the CD spectra of **elastin-3**, with the exception that the onset of the conformational transition occurs at a lower temperature and that a more fully developed β -turn conformation is observed at higher temperatures. In contrast, the CD spectra of **elastin-2** differ significantly from those of the other two elastin-mimetic polypeptides in that evidence of an alternative conformation is detected even at lower temperatures as a shoulder at approximately 220 nm on the major absorbance. In addition, the CD minimum associated with the random coil absorption is shifted to slightly higher wavelengths in comparison to those of **elastin-1** and **elastin-3**. As the random coil signature diminishes at higher temperatures, the longer wavelength feature dominates the CD spectra of **elastin-2**. A weak positive ellipticity is also observed near 208 nm in the CD spectra of **elastin-2** at higher temperatures that might indicate the presence of a type II β -turn conformation. However, the breadth of the CD traces observed at higher temperatures suggests that the (VPGVG) repeat unit significantly populates alternative conformations in addition to a type II β -turn (vide infra) as the temperature approaches the transition point. Indeed, the thermal transition curves for the disappearance of the random coil conformation, as judged by the change in mean residue ellipticity at the wavelength associated with the random coil

(36) Makhatadze, G. I. *Biophys. Chem.* **1998**, *71*, 133–156.

(37) Cooper, A. *Biophys. Chem.* **2000**, *85*, 25–39.

(38) (a) Urry, D. W.; Luan, C.-H.; Parker, T. M.; Gowda, D. C.; Prasad, K. U.; Reid, M. C.; Safavy, A. *J. Am. Chem. Soc.* **1991**, *113*, 4346–4347. (b) Urry, D. W.; Gowda, D. C.; Parker, T. M.; Luan, C.-H. *Biopolymers* **1992**, *32*, 1243–1250.

(39) Meyer, D. E.; Chilkoti, A. *Biomacromolecules* **2004**, *5*, 846–851.

(40) Yamaoka, T.; Tamura, T.; Seto, Y.; Tada, T.; Kunugi, S.; Tirrell, D. A. *Biomacromolecules* **2003**, *4*, 1680–1685.

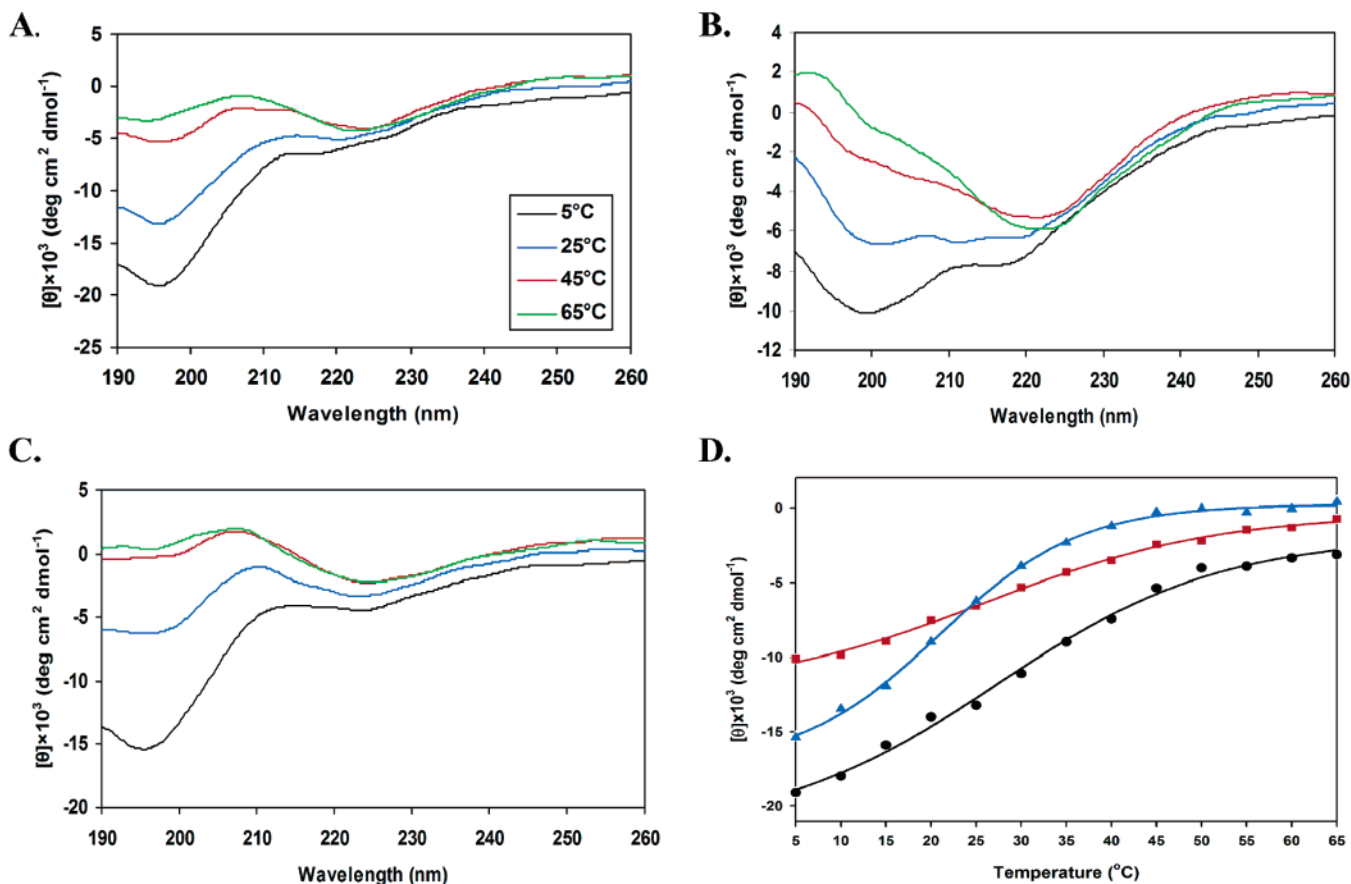


Figure 2. (A, B, and C) Circular dichroism spectral manifolds depicting the thermally induced conformational transitions for the polypeptides **elastin-1**, **elastin-2**, and **elastin-3**, respectively, at representative temperatures within proximity of the phase transition. (D) Thermal transition profiles monitoring the disappearance of the random coil conformation ($[\Theta]_{195}$) in the CD spectra of **elastin-1** (black), **elastin-2** (red), and **elastin-3** (blue).

minimum, $[\Theta]_{195}$, suggest the presence of a two-state transition for **elastin-1** and **elastin-3**, but not for **elastin-2**, under the experimental conditions (Figure 2D). The mathematical fits of the thermal transitions for **elastin-1** and **elastin-3** provided estimates for the respective transition temperatures (T_i) of 29.1 °C and 22.8 °C that approximate the corresponding T_i values calculated from DSC measurements of the respective polypeptides.⁴⁰

Similar structural analyses of modified collagen-mimetic peptides suggested that the molecular origin of the observed differences in thermodynamic and conformational properties between the elastin analogues might be rationalized in terms of the stereoelectronic effect of the *fluoro* substituents on the conformation of the pyrrolidine ring, particularly as it affects the local secondary structure of the polypeptide.^{2–5} These stereoelectronic effects might be manifested within the elastin structure either through the influence of the pyrrolidine ring pucker on the *cis/trans* conformational equilibrium of the Val-Pro peptide bond, through its influence on the local (ϕ, ψ) torsional angles of the proline residue, or through a combination of the two effects.¹ Two-dimensional ^1H – ^1H NOESY NMR spectroscopy of the elastin-mimetic polypeptides indicated that the major peptidyl bond conformation corresponded to the *trans* isomer as detected through the strong Val(H α)-Pro(H δ) correlation for all three elastin analogues (cf. Supporting Information).⁴¹ Minor peaks corresponding to the *cis* isomer of the Val-

Pro peptide bond could be identified for **elastin-2**. However, even in the latter situation, in which the (4*S*)-fluoroproline should display a greater propensity for the *cis* prolyl peptide bond isomer,^{8,21} the integrated intensity of the minor peaks corresponded to less than 20% of the total peptide pool. Similarly, the previously reported ^{19}F NMR spectra of **elastin-2** and **elastin-3** provided evidence for the presence of a minor *cis*-peptidyl isomer at a fractional content consistent with that observed from the respective ^1H NMR spectra.¹⁸ The strong preference for the *trans* prolyl peptide bond isomer within these elastin derivatives coincides with the previously described propensity of Xaa-Pro peptidyl bonds to favor the *trans* orientation when the preceding residues have β -branched side chains such as the valine residues within the elastin repeats.⁴² Although, especially in the case of **elastin-2**, the presence of a *cis* Val-Pro peptidyl bond isomer may play a minor role in the conformational equilibria that influence the elastin assembly, the NOESY-NMR spectroscopic data suggest that the observed differences in the macromolecular properties between these elastin derivatives detected from CD and DSC studies do not arise primarily as a consequence of prolyl peptidyl bond isomerism.

Alternatively, stereoelectronic effects on protein structure can stem from the influence of the pyrrolidine ring pucker on the local (ϕ, ψ) angles of the proline residue. Despite the structural similarity of (4*S*)- and (4*R*)-fluoroproline, the stereoelectronic

(41) Andreotti, A. H. *Biochemistry* **2003**, *42*, 9515–9524.

(42) Reimer, U.; Scherer, G.; Drewello, M.; Kruber, S.; Schutkowski, M.; Fischer, G. *J. Mol. Biol.* **1998**, *279*, 449–460.

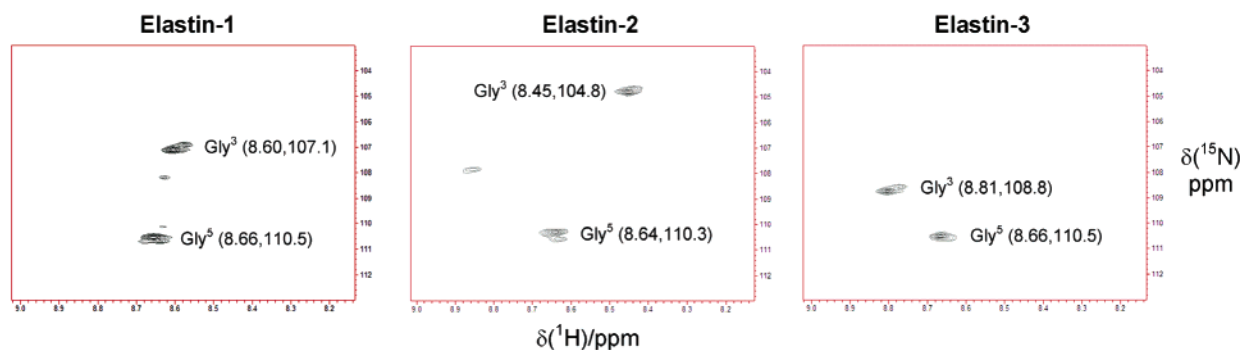


Figure 3. Comparison of the ^1H - ^{15}N HSQC NMR spectra of **elastin-1**, **elastin-2**, and **elastin-3**, indicating the positions of the chemical shifts associated with the glycine residues that occur in the repetitive domain. Spectra were acquired at 4 °C as described in the Experimental Section on elastin specimens that had been labeled with ^{15}N at the amide positions corresponding to nonproline residues, i.e., valine, glycine, and isoleucine, within the repetitive domains of the polypeptides. The unlabeled cross-peaks in the spectra correspond to minor species that might be associated with the presence of *cis*-peptidyl isomers of the Val-Pro bond and, consequently, do not show correlations to the major *trans*-peptidyl bond isomer under the experimental conditions.

fluorine-amide gauche effect alters the preferred ring pucker between the two isomers, which is manifested in subtle but distinct differences in the thermodynamic preferences of the main chain dihedral angles associated with the proline residue. Computational investigations of the methyl esters of the *N*-acetyl-4-fluoroproline epimers have shown significant differences in the dependence of the conformational energy on the value of the dihedral angle ψ , particularly notable for the (4*S*)-fluoroproline derivative in the *C'*-endo pucker of the pyrrolidine ring.¹ We suggest that the differences in macro-molecular behavior observed among the elastin analogues can be interpreted in terms of the closeness of correspondence between the preferred values of the ψ angle for the substituted proline derivatives and the preferred range of ψ angles associated with proline residues in the ($i + 1$) position of a type II β -turn conformation (ideal $\beta_{\text{II}} \phi, \psi$: -60° , 120°). Prior structural investigations of elastin-mimetic polypeptides have demonstrated that the phase transition is closely associated with the formation of type II β -turn structures within the pentapeptide repeats, in which the Pro²-Gly³ residues of the repeats occupy the ($i + 1$) and ($i + 2$) positions of the turn sequence, respectively.^{12–17} A crystallographic structural determination on the model elastin peptide, *cyclo*-(VPGVG)₃,²⁴ indicated that the (ϕ, ψ) dihedral angles observed for the proline residues, (-53° , 140°), are within the expected range for the ($i + 1$) position of a type II β -turn conformation. We noted above that the conformation of the pyrrolidine rings of proline residues within the crystal structure of *cyclo*-(VPGVG)₃ corresponds to a *C'*-exo pucker. Significantly, the minimal energy dihedral angles calculated for the *exo* isomer of the model compound, Ac-(4*R*)-F-Pro-OMe (-59.22° , 140.79°),¹ closely correspond to those observed for the proline residues in the crystal structure of *cyclo*-(VPGVG)₃. In contrast, the unsubstituted proline residue displays a slight thermodynamic preference for the *C'*-endo ring pucker, in which the dihedral angles diverge from those preferred for a type II β -turn.^{1,8} Thus, a stereoelectronic effect may preorganize the conformation of the (4*R*)-fluoroproline residues in **elastin-3** for the transition to a type II β -turn, thereby facilitating the self-assembly process vis-à-vis **elastin-1**.

How then can one explain the anomalous conformational behavior of **elastin-2**? The (4*S*)-fluoroproline residue displays a strong thermodynamic preference for the *C'*-endo ring pucker as a consequence of the gauche effect between the vicinal fluorine and amide substituents.^{1,8,21–23} However, computational

studies of the conformational energetics for the model compound Ac-(4*S*)-F-Pro-OMe indicated that a 1,3-diaxial interaction between the fluoro and carboxyl substituents on the pyrrolidine ring significantly distorts the minimal energy values of the (ϕ, ψ) angles for the substituted proline residue in the *C'*-endo conformation (-76.44° , 171.95°)¹ away from the typical values of the ψ angle associated with the type II β -turn conformation. In addition, calculations of total energy and steric exchange energy versus ψ for fragments derived from this model compound exhibited energetic maxima at values of ψ corresponding to those associated with the type II β -turn conformation. Taken in combination, these considerations suggest that the *C'*-endo pucker of pyrrolidine ring in (4*S*)-fluoroproline energetically destabilizes the type II β -turn structure relative to alternative conformations that are energetically accessible for the pentapeptide repeats, which results in the elevated transition temperature and anomalous conformational behavior observed for **elastin-2**.

Complementary spectroscopic evidence suggests that significant conformational differences occur between the **elastin-2** and **elastin-3**, which presumably originate from an altered population of pyrrolidine ring conformers among the substituted proline residues. Conformational information regarding the local environment about the proline residue can be gleaned from the ^1H - ^{15}N HSQC NMR spectra of the elastin analogues (Figure 3). The ^1H and ^{15}N chemical shifts of the Gly³ amide group should depend strongly on the ψ angle of the preceding proline residue^{43,44} and, therefore, should be sensitive to local structural perturbations that arise from stereoelectronic effects. The values of these chemical shifts depend dramatically on the identity of the proline derivative within the elastin-mimetic polypeptide. The ^1H and ^{15}N chemical shifts of Gly³ are displaced to high field for **elastin-2** and to low field for **elastin-3** relative to the corresponding chemical shift values for **elastin-1**. These shifts reflect incipient structural development within the Pro²-Gly³ structural unit, which even at 4 °C does not correspond to a completely denatured random coil conformation on the basis of the values of $[\Theta]_{195}$ observed in the CD spectra (Figure 2).^{15,45} We may infer from the observed distribution of Gly³ chemical shifts among the elastin analogues that the Pro² residues experience different conformational environments even at

(43) Wishart, D. S.; Nip, A. M. *Biochem. Cell Biol.* **1998**, *76*, 153–163.

(44) Le, H.; Oldfield, E. J. *Biomol. NMR* **1994**, *4*, 341–348.

(45) Provencher, S. W.; Glockner, J. *Biochemistry* **1981**, *20*, 33–37.

temperatures below the respective transition points. In contrast, the values of the ^1H and ^{15}N chemical shifts for the Gly⁵ amide group, which does not participate in the incipient β -turn conformation, do not significantly vary among the elastin derivatives. The downfield displacement of the Gly³ ^{15}N and ^1H chemical shifts for **elastin-3** with respect to the corresponding resonances of **elastin-1** is consistent with increased occupancy of the type II β -turn conformation on the basis of empirical chemical shift correlations.^{43,44} However, the observed upfield shift of the ^1H and ^{15}N resonances derived from the Gly³ residues in the HSQC NMR spectra of **elastin-2** cannot be interpreted in terms of chain conformations commonly associated with the elastin pentapeptide repeats on the basis of spectroscopic^{12,15} and computational¹⁶ analyses and may reflect with increased occupancy of alternative turn structures in which the local conformation of the proline residue is shifted toward less positive values of the ψ angle. Arad and Goodman have described an equilibrium between β -turn and γ -turn conformations within the pentapeptide repeats on the basis of spectroscopic analyses of elastin-mimetic peptides.⁴⁶ The relative population of the γ -turn conformation can be increased in depsipeptide analogues of the pentapeptides in which Val⁴ has been replaced with the non-hydrogen bonding isostere, 2-hydroxyisovaleric acid. In addition, molecular dynamics simulations of (Val-Pro-Gly-Val-Gly)₁₈ at temperatures above the transition point provide evidence for a minor population of proline residues with negative ψ values that are consistent with type I β -turn structures.¹⁶ The CD and NMR spectroscopic data for **elastin-2** suggest that the presence of the (4*S*)-fluoroproline residue may tip the conformational equilibria of the pentapeptide repeats toward alternative turn structures, vis-à-vis **elastin-1** and **elastin-3**, through a relative destabilization of the type II β -turn conformation. The upfield chemical shift of the ^{15}N signal for the Gly³ amide of **elastin-2** is consistent with a greater population of type I β -turn structures based on the calculated ^{15}N chemical shifts for different turn structures of the model turn segment (MeCO-Xaa-Gly-NHMe) (vide infra) and empirical ^{15}N chemical shift correlations. In addition, the CD spectra of **elastin-2** display an increase in the magnitude of the negative ellipticity absorption at 222 nm near the phase transition, which occurs at the expense of the positive ellipticity absorption at 207 nm associated with type II β -turn formation. Qualitative comparison of the CD spectra of the elastin peptides to conformational deconvolutions of the CD spectra of model type I and type II β -turn structures⁴⁷ suggests that the observed difference in CD spectroscopic behavior for **elastin-2** may be attributable to an increase in type I β -turn conformation relative to type II β -turn conformation with respect to **elastin-1** and **elastin-3**. Taken together, the spectroscopic data may indicate that the relative populations of the different turn structures associated with the conformational transition of the (VPGVG) units depends on the structural identity of the proline analogue and can be rationalized on the basis of stereoelectronic effects.

Computational Studies of (Pro-Gly) Turns. To assist interpretation of the structural consequences of introduction of (4*S*)-fluoroproline versus (4*R*)-fluoroproline into these elastin-mimetic polypeptides, we have used density functional theory

Table 1. Calculated Values for Energy Differences (ΔE , kcal/mol), ϕ, ψ Angles (deg), and ^{15}N Chemical Shifts (ppm) for Type-I β -turns, Type-II β -turns, and Inverse γ -Turns in the Truncated Turn Model (MeCO-Xaa-Gly-NHMe) (Xaa = Pro, 4*S*-F-Pro, 4*R*-F-Pro)

β_I turn	total E , au ^a	ΔE	Pro ϕ and ψ ^b	Gly ϕ and ψ ^b	δ (N-H) ^c
<i>exo</i>	-781.530 155	0.4	-66.8, -18.8	-97.5, 10.2	95.1, ^d 105.9 ^e
<i>endo</i>	-781.530 807	0.0	-78.3, -3.7	-99.8, 7.8	102.1, ^d 113.8 ^e
<i>exo</i> -F _{eq}	-880.798 527	1.8	-68.1, -18.1	-97.3, 10.3	95.4, ^d 106.0 ^e
<i>endo</i> -F _{ax}	-880.801 461	0.0	-74.1, -8.9	-103.1, 10.4	100.5, ^d 111.5 ^e
<i>exo</i> -F _{ax}	-880.801 367	0.0	-70.5, -15.1	-97.5, 9.5	96.4, ^d 107.5 ^e
<i>endo</i> -F _{eq}	-880.799 024	1.6	-78.5, -2.8	-100.3, 7.8	95.1, ^d 105.9 ^e
β_{II} turn	total E , au ^a	ΔE	Pro ϕ and ψ ^b	Gly ϕ and ψ ^b	δ (N-H) ^c
<i>exo</i>	-781.533 453	0.0	-57.7, 127.5	99.8, -14.2	111.7, ^d 122.7 ^e
<i>endo</i>	-781.533 325	0.08	-65.1, 126.3	97.2, -10.0	110.8, ^d 121.8 ^e
<i>exo</i> -F _{eq}	-880.801 957	0.0	-58.8, 127.1	100.1, -13.7	112.2, ^d 123.2 ^e
<i>endo</i> -F _{ax}	-880.799 121	1.8	-61.0, 133.1	97.7, -15.2	109.1, ^d 120.6 ^e
<i>exo</i> -F _{ax}	-880.805 750	0.0	-60.1, 124.9	100.6, -12.9	113.1, ^d 123.9 ^e
<i>endo</i> -F _{eq}	-880.803 256	1.6	-65.5, 125.3	99.9, -10.9	112.1, ^d 123.1 ^e
i - γ turn	total E , au ^a	ΔE	Pro ϕ and ψ ^b	Gly ϕ and ψ ^b	δ (N-H) ^c
<i>exo</i>	-781.530 860	1.0	-82.0, 76.6	-122.1, 14.4	111.8, ^d 125.5 ^e
<i>endo</i>	-781.532 457	0.0	-83.7, 72.7	-121.5, 14.8	110.5, ^d 124.0 ^e
<i>exo</i> -F _{eq}	-880.799 711	0.1	-82.4, 76.8	-115.5, 9.8	113.5, ^d 125.0 ^e
<i>endo</i> -F _{ax}	-880.799 937	0.0	-81.6, 54.3	-107.6, 8.7	107.7, ^d 121.3 ^e
<i>exo</i> -F _{ax}	-880.803 764	0.0	-83.5, 76.6	-116.0, 9.3	111.6, ^d 125.0 ^e
<i>endo</i> -F _{eq}	-880.801 745	1.3	-84.0, 76.1	-113.4, 7.8	111.2, ^d 124.4 ^e

^a Beck3LYP/6311+G(2d,p)//Beck3LYP/6-311+G*. ^b ϕ angle (O)C-N-C-C(O); ψ angle N-C-C(O)-N. ^c Calculated ^{15}N chemical shifts for N-H bonds of the Gly residue of (MeCO-Xaa-Gly-NHMe) in ppm relative to liquid NH₃ at 25 °C (absolute shielding 244.6 ppm is set to 0 ppm); see Experimental Section for details. ^d MPW1PW91/6-311G*/Beck3LYP/6-311+G*. ^e PBE/6-311+G(2d,p)//Beck3LYP/6-311+G*.

(DFT) to model three possible turn types (β_I , β_{II} , and inverse γ) derived from peptide segments corresponding to the turn-forming residues of the elastin repeat unit (VPGVG). The pentapeptide repeat unit was truncated to a capped moiety corresponding to the turn fragment (MeCO-Xaa-Gly-NHMe) (Xaa = Pro, 4*S*-F-Pro, 4*R*-F-Pro). The proline envelope conformations were placed in conformational equilibrium by virtue of a flip of the five-membered pyrrolidine ring of the proline residue between the *exo* and *endo* orientations. For ease of discussion here and in connection with Table 1, the (4*R*)-pair of conformers have been designated *exo*-F_{ax} and *endo*-F_{eq}, in which the *exo*-F_{ax} implies a *C*^γ-*exo* orientation of the proline ring with an axial disposition of the C-F bond. The (4*S*)-pair of conformers, *exo*-F_{eq} and *endo*-F_{ax}, are similarly characterized by equilibrating pyrrolidine ring pucker isomers. The three parent turns and the six 4-fluorinated turn structures were optimized in *C*^γ-*exo* and *C*^γ-*endo* conformations with both double- ζ and enhanced triple- ζ basis sets (6-31G* and 6-311+G*, respectively) in order to define the computational requirements for adequately describing the various turns. Supplemental energy differences were obtained using the triple- ζ basis set with extensive polarization (i.e., 6-311+G(2d,p)). The Becke3LYP/6-31G* optimizations (cf. Supporting Information) were performed both to obtain preliminary structures for the 6-311+G* refinements and to evaluate whether they might be sufficiently predictive for this class of problem. As it concerns molecular geometry, the Becke3LYP/6-31G* spread of ϕ, ψ angles is satisfactory, though in some cases a bit broader than derived at the 6-311+G* basis set level. Energetically, when the 6-31G* optimized structures are re-evaluated with the Becke3LYP/6-311+G(2d,p) model, conformational energy differences are routinely within 0.2 kcal/mol by comparison with structures

(46) Arad, O.; Goodman, M. *Biopolymers* **1990**, *29*, 1652-1668.

(47) (a) Perczel, A.; Hollosi, M.; Sandor, P.; Fasman, G. D. *Int. J. Pept. Protein Res.* **1993**, *41*, 223-236. (b) Perczel, A.; Kollat, E.; Hollosi, M.; Fasman, G. D. *Biopolymers* **1993**, *33*, 665-685.

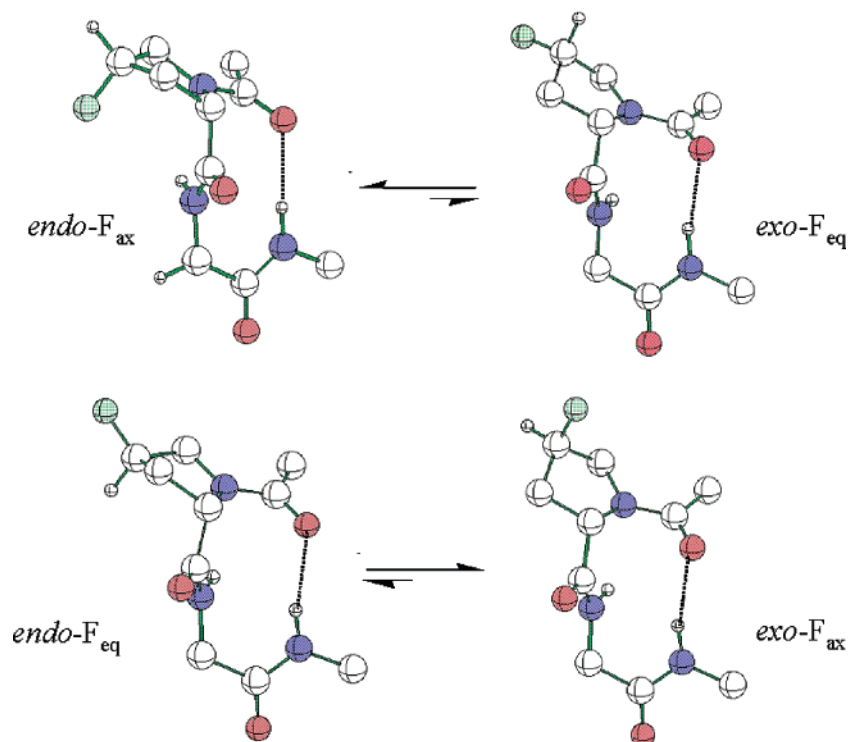


Figure 4. Calculated structures of conformer pairs for type I β -turn structures derived from the model peptide segment (MeCO-Xaa-Gly-NHMe) incorporating (2*S*,4*S*)-4-fluoroproline (top) and (2*S*,4*R*)-4-fluoroproline (bottom). The labels indicate the ring pucker associated with the C γ position of the pyrrolidine ring and the position of the fluorine substituent. Geometries were derived from structural optimization at the Beck3LYP/6311+G(2d,p) level of theory.

optimized at 6-311+G* (cf. Supporting Information). For both parent and fluorinated prolines, the conformational forms for (MeCO-Xaa-Gly-NHMe) (Xaa = Pro, 4*S*-F-Pro, 4*R*-F-Pro) posit ϕ and ψ torsional angles for the proline and glycine residues that are within 30° of the ideal ($\phi_1\psi_1\phi_2\psi_2$) values corresponding to the (i+1) and (i+2) residues of the respective turn type (Table 1).^{48,49} However, the relative energetic stabilities associated with turn formation display striking differences between ring pucker conformations for the fluoroproline derivatives of the model peptide segment (Table 1).

The DFT 6-311+G(2d,p) energies suggest that the type I β -turn structures corresponding to *endo*-F_{ax} and *exo*-F_{ax} conformers are the more stable species for (4*S*)- and (4*R*)-fluoroproline derivatives, respectively (Table 1 and Figure 4). Taken at face value, the observed energy differences of 1.8 and 1.6 kcal/mol for the *endo*-F_{ax} and *exo*-F_{ax} conformers vis-à-vis their conformational partners suggest 95% and 94% populations, respectively, for these low energy forms at 298 K. The observed conformational preferences of the (4*S*)- and (4*R*)-fluoroproline derivatives in these type I β -turn structures reflect the conformational preferences for the C γ -*endo* and C γ -*exo* isomers, respectively, that had been previously reported from structural studies of the corresponding substituted proline derivatives (vide supra). In both preferred ring pucker conformations, the C–F bond has an axial orientation with respect to the pyrrolidine ring. Previous experimental studies of fluorinated proline derivatives suggested that the primary driving force for this puckering outcome could be ascribed to the fluorine-amide gauche effect and to favorable hyperconjugation between *trans*-

disposed C–F and C–H bonds.^{1,2,20,21} These structural criteria are applicable for rationalizing the stability of the *endo*-F_{ax} and *exo*-F_{ax} conformations within the type I β -turns of (4*S*)- and (4*R*)-fluoroproline-substituted (MeCO-Pro-Gly-NHMe) units, respectively, as the preferred conformer in each case incorporates both of these structural features.

The results obtained for the type I β -turn structures can be compared to the corresponding features calculated for the type II β -turns (Table 1 and Figure 5). Energetically, the C γ -*endo* and C γ -*exo* conformers of the proline-containing parent turns derived from the (MeCO-Pro-Gly-NHMe) unit are within 0.1 kcal/mol (54% (*exo*)/46% (*endo*) populations, 298 K). Note that the very slight energetic difference between the two ring puckers for the unsubstituted (MeCO-Pro-Gly-NHMe) unit in a type II β -turn structure stands in direct contrast to the single ring pucker conformation observed for proline residues in the crystal structure of *cyclo*-(VPGVG)₃.²⁴ This discrepancy suggests that the observed C γ -*exo* preference in the latter structure may have arisen from a combination of nonlocal structural considerations distinct from turn formation, including, but not limited to, crystal packing forces, turn catenation, and peptide backbone cyclization. In contrast with the computational results obtained for the type I β -turn system, fluoroproline substitution within type II β -turn structures favors the C γ -*exo* proline conformers, *exo*-F_{eq} and *exo*-F_{ax}, for the (4*S*)- and (4*R*)-fluoroproline derivatives, respectively, with populations predicted to be in the 94–95% range according to the Beck3LYP/6-311+G(2d,p) calculations. The stability of the (4*R*)-*exo*-F_{ax} form can be attributed to the gauche effect and C–H/C–F hyperconjugation as described above; however, the (4*S*)-*exo*-F_{eq} conformation can take advantage of neither of these effects. We suggest that the source of the relative energies between ring pucker conformers associ-

(48) Wilmot, C. M.; Thornton, J. M. *J. Mol. Biol.* **1988**, *203*, 221–232.

(49) (a) Rose, G. D.; Gierasch, L. M.; Smith, J. A. *Adv. Protein Chem.* **1985**, *37*, 1–109. (b) Milner-White, E. J.; Ross, B. M.; Ismail, R.; Belhadj-Mastefa, K.; Poet, R. *J. Mol. Biol.* **1988**, *204*, 777–782.

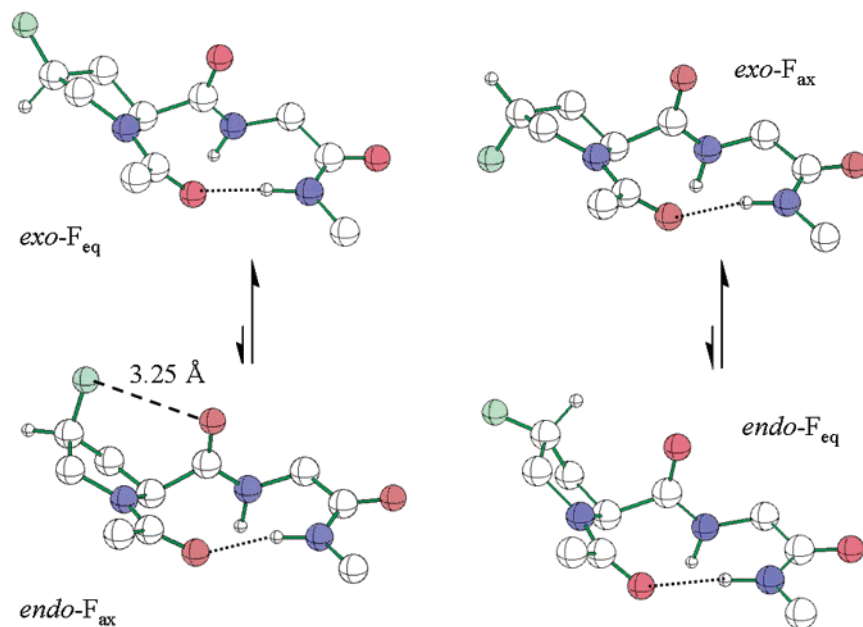


Figure 5. Calculated structures of conformer pairs for type II β -turn structures derived from the model peptide segment (MeCO-Xaa-Gly-NHMe) incorporating (2*S*,4*S*)-4-fluoroproline (left) and (2*S*,4*R*)-4-fluoroproline (right). The labels indicate the ring pucker associated with the C^γ position of the pyrrolidine ring and the position of the fluorine substituent. The contact distance between axially disposed C–F and C–O bond vectors is depicted for the *endo-F_{ax}* isomer of (MeCO-4*S*-F-Pro-Gly-NHMe). Geometries were derived from structural optimization at the Beck3LYP/6311+G(2d,p) level of theory.

ated with (4*S*)-fluoroproline lies in the energetic instability of the *endo-F_{ax}* conformational partner. As depicted in Figure 5, the C–F bond is apposed to the central amide's C=O bond in the *endo-F_{ax}* conformer with the F and O atoms separated by 3.25 Å. While this distance does not violate the sum of the van der Waals boundaries (2.99 Å),⁵⁰ it is sufficiently short to bring the nonbonding electron lone pairs from each atom into juxtaposition. We presume that the accompanying lone-pair/lone-pair repulsion is sufficient to override both *gauche* and hyperconjugation effects for the axial fluorine in (4*S*)-*endo-F_{ax}* conformation, thereby raising its energy relative to (4*S*)-*exo-F_{eq}*. The distortion of the (4*S*)-*endo-F_{ax}* conformer in a type II β -turn structure can be inferred from deviations in the values of ($\phi_1\psi_1\phi_2\psi_2$) dihedral angles associated with the (MeCO-4*S*-F-Pro-Gly-NHMe) unit, particularly ψ_1 of proline (133.1°), in comparison to the corresponding values for the C^γ -*endo* conformers of the other proline derivatives (Table 1). In this context, it is noteworthy that, while (4*S*)-*exo-F_{eq}* is predicted to be thermochemically more stable than the (4*S*)-*endo-F_{ax}* conformer, the equatorial structure is calculated to be 2.3 kcal/mol *less stable* than the (4*R*)-*exo-F_{ax}* epimer associated with (4*R*)-fluoroproline in the type II β -turn structures predicted for MeCO-4*R*-F-Pro-Gly-NHMe.

For a comparison of relative energies between the various turn conformations within the model peptide segment (MeCO-Xaa-Gly-NHMe) (Xaa = Pro, 4*S*-F-Pro, and 4*R*-F-Pro), we consider the values observed for the most stable forms recorded under ΔE in Table 1. For the unsubstituted parent peptide, the type II β -turn conformation is the most stable, with a very slight preference for the C^γ -*exo* conformation. Similarly, for the model peptide segment (MeCO-4*R*-F-Pro-Gly-NHMe), the *exo-F_{ax}* conformer of the type II β -turn is predicted to be lowest in energy and, indeed, is the most energetically stable conformation by 2.4–3.6 kcal/mol among all of the turn sequences under

consideration in this study. Notably, the C^γ -*exo* isomers comprise the most stable conformations for all turns involving (4*R*)-fluoroproline, which provides a dramatic example of the influence of stereoelectronic control within this structural context. In addition, the order of relative stabilities among the turn sequences are similar for the parent peptide and the (4*R*)-fluoroproline derivative in that the energies of the most stable conformers are ordered such that $\beta_{II} < \gamma < \beta_I$. For the (MeCO-4*R*-F-Pro-Gly-NHMe) model peptide system, the computational data indicate a greater stabilization of the type II β -turn structure with respect to alternative turns (Table 1) than for proline within the model peptide system, which provides support for the hypothesis that experimental differences observed between **elastin-1** and **elastin-3** may arise as a consequence of stereoelectronic influences within the (VPGVG) structural context. However, given the assumptions in truncating VPGVG, the absence of solvent in the calculations, and, most importantly, the absence of any elastin protein environment, it is reasonable to assume that all of the turn forms are energetically accessible to the elastin polypeptides under experimentally relevant conditions, as is suggested from spectroscopic investigations⁴⁶ and molecular dynamics simulations¹⁶ of elastin-mimetic model peptides.

In contrast to the stereoelectronic control observed for turns involving the (4*R*)-fluoroproline epimer, we find that the C^γ -*endo* isomer of (4*S*)-fluoroproline, which should be preferred on the basis of stereoelectronic considerations associated with fluorine substitution, is not necessarily the most stable conformation in turn sequences derived from the model peptide segment (MeCO-4*S*-F-Pro-Gly-NHMe). For the type II β -turn structure, the C^γ -*exo* isomer corresponds to the energetically most favorable pucker of the pyrrolidine ring even though this conformational arrangement cannot gain stabilization from either a stereoelectronic *gauche* effect or C–H/C–F hyperconjugation.^{2,8} However, as mentioned above, significant energetic

(50) Bondi, A. J. *Phys. Chem.* **1964**, *68*, 441–451.

destabilization of the C^γ -endo isomer may arise vis-à-vis the C^γ -exo isomer due to lone-pair/lone-pair repulsion between the axial F and O atoms of the pyrrolidine ring within the (4*S*)-fluoroproline (Figure 5). A computational analysis of the conformational energetics of the *N*-acetyl, methyl ester derivative of (4*S*)-fluoroproline suggested that significant energetic destabilization of the C^γ -endo isomer was associated with particular values of the dihedral angle ψ .¹ We note from these results that the energetic destabilization of the C^γ -endo isomer of a (4*S*)-fluoroproline-derived structural fragment was pronounced at ψ values near the preferred ψ range for the ($i + 1$) residue of type II β -turn structures that would be occupied by the substituted proline. A corresponding energetic destabilization was not observed for C^γ -exo isomer of (4*S*)-fluoroproline at similar values of the dihedral angle ψ . Taken together, these computational data suggest that certain secondary structures, e.g., the type II β -turn, that place the value of the ψ angle for the (4*S*)-fluoroproline residue within this unfavorable region would energetically destabilize the C^γ -endo isomer versus the C^γ -exo isomer, thus negating the stereoelectronic influence of the fluorine substituent. The presence of (4*S*)-fluoroproline effectively raises the energy of the type II β -turn structures for the model peptide (MeCO-4*S*-F-Pro-Gly-NHMe) such that other turns, particularly the type I β -turn structure, become more similar in energy (Table 1). Note that the computational data indicate a trend in which the difference in energy between the β_{II} and β_I turns (ΔE_{II-I}) decreases in the model peptide series (MeCO-Xaa-Gly-NHMe) from Xaa = 4*R*-F-Pro (2.8 kcal mol⁻¹) to Pro (1.7 kcal mol⁻¹) to 4*S*-F-Pro (0.3 kcal mol⁻¹). Thus, computational analyses of the model peptide segment (MeCO-Xaa-Gly-NHMe) suggest that the differences in spectroscopic and calorimetric behavior between the corresponding elastin derivatives, in particular, the discrepancy in transition temperature and variation in type II β -turn content observed between **elastin-3** vis-à-vis **elastin-2**, can be rationalized on the basis of differential stereoelectronic stabilization of the incipient type II β -turn structure as the temperature approaches the phase transition. While the calculated energetic differences between turn structures in the model system are relatively small for all three proline derivatives, this situation does not preclude the possibility that the relative populations of the various turn structures under consideration might be constituted in a manner that can account for the observed differences in physical characteristics between **elastins-1**, **-2**, and **-3**.

To draw a closer correlation between the computational data and the experimental results derived from structural characterization of the series of elastin-mimetic peptides, we computed the values of the ¹⁵N chemical shifts for the structurally sensitive Gly amide groups (cf. Experimental Section) of the model peptide segment (MeCO-Xaa-Gly-NHMe) (Xaa = Pro, 4*S*-F-Pro, and 4*R*-F-Pro) in different turn structures and ring pucker conformations (Table 1). While differences are observed between the calculated ¹⁵N-Gly chemical shifts for the (MeCO-Xaa-Gly-NHMe) units and the experimental chemical shifts for structurally analogous Gly³ of the elastin-mimetic polypeptides (due to presumed differences in the environment of the peptides, gas phase and aqueous solution, respectively), nonetheless the trends are consistent with predictions based on comparison of the calculated chemical shifts with empirical correlations for the amide groups of polypeptides.^{43,44} Significantly, the com-

putational data indicate that the type II β -turn structure of the (MeCO-Xaa-Gly-NHMe) unit typically results in a downfield shift of the amide ¹⁵N signals for the ($i + 2$) Gly residue in comparison to the corresponding type I β -turn structure regardless of the ring pucker conformation (Table 1). The MPW1PW91/6-311G* ¹⁵N chemical shifts calculated for (MeCO-4*R*-F-Gly-NHMe) and (MeCO-Pro-Gly-NHMe), both presumed to sustain a type-II β -turn in analogy to **elastin-3** and **elastin-1**, are 113.1 (*exo*-F_{ax}) and 111.3_{avg} ppm, respectively (Table 1). As the C^γ -exo and C^γ -endo conformers of (MeCO-Pro-Gly-NHMe) are isoenergetic, the latter value is an average of these two conformers. The predicted shifts are not only within 4–5 ppm of the measured values, but both the ordering and differences ($\Delta\delta(^{15}\text{N}) = 1.7(\text{expt})$ and $1.8(\text{calcd})$ ppm, respectively) are accurately modeled. The PBE functional predicts the values to be low-field shifted by an additional 10 ppm, but once again both the ordering and difference ($\Delta\delta(^{15}\text{N}) = 1.1$ ppm) matches experiment. Both chemical shift estimates support the assignment of type II β -turn as the preferred structure for the VPGVG units of **elastin-1** and **elastin-3**.

In contrast, the computational data indicate that the significant upfield shift of the amide ¹⁵N signals of the Gly³ residue of **elastin-2** may occur as a consequence of a potentially higher population of alternative turn structures, in particular, the type I β -turn, that arise at the expense of the type II β -turn population. MPW1PW91/6-311G* calculations for the more stable (4*S*)-endo-F_{ax} conformer of the type-I β -turn predicted a sizable upfield ¹⁵N shift of 100.5 ppm (Table 1, $\Delta\delta(^{15}\text{N}) = 11.0$ (calcd) ppm) with respect to the corresponding type II β -turn structure. Although the calculated shift difference for (MeCO-4*S*-F-Pro-Gly-NHMe) is more substantial than that observed experimentally between the elastin-mimetic polypeptides, the former assumes that the model structures define uniform populations of turn conformations. Computational analyses of the relative energetics of the turn structures for (MeCO-4*S*-F-Pro-Gly-NHMe) suggest that the type II β -turn becomes destabilized relative to alternative turn structures in comparison to the other proline derivatives, although it remains the most stable turn under the constraints of the analysis (Table 1). The calculations imply an altered equilibrium population of turn species for **elastin-2** relative to **elastin-1** and **elastin-3**, which may manifest itself in the upfield chemical shift of Gly³ ¹⁵N of **elastin-2** with respect to the other elastin derivatives. As suggested in the discussion of the ¹H–¹⁵N HSQC NMR spectra of the elastin derivatives, the trend in observed Gly³ ¹⁵N NMR spectral shifts for the elastin-mimetic polypeptides indicates a decrease in type II β -turn content from **elastin-3** (108.8 ppm) to **elastin-1** (107.1 ppm) to **elastin-2** (104.8 ppm), which coincides qualitatively with the trend in relative energies between β_{II} and β_I turns calculated for the corresponding model peptides.

Conclusion

The experimental data derived from calorimetric and spectroscopic analyses of **elastin-1**, **elastin-2**, and **elastin-3** provide evidence that stereoelectronic effects may alter the self-assembly of elastin-mimetic polypeptides, and, by inference, native elastin, through their influence on the local conformation parameters of the β -turn structures that develop in the structural repeats above the phase transition. Moreover, the observed differences in macromolecular behavior between the elastin derivatives reinforce the hypothesis that type II β -turn formation plays an

important role in elastin assembly, as previously postulated from spectroscopic and computational analyses of elastin-mimetic polypeptides.^{12–17} For the elastin-mimetic polypeptides under consideration in this study, structural factors that increase the stability of the type II β -turn structure of the (VPGVG) unit, i.e., stereoelectronic stabilization due to incorporation of (4*R*)-fluoroproline into **elastin-3**, resulted in a lower transition temperature for elastin assembly. Conversely, structural factors that decrease the stability of the type II β -turn structure of the (VPGVG) unit, such as incorporation of (4*S*)-fluoroproline into **elastin-2**, raised the transition temperature of elastin assembly. Computational analyses of the conformational energetics associated with various turn structures (β_I , β_{II} , inverse γ) of the model peptide (MeCO-Xaa-Gly-NHMe) unit (Xaa = Pro, 4*S*-F-Pro, 4*R*-F-Pro) suggest that the relative stability of the conformers depends on the effect of the proline derivative on the metrical parameters associated with the local polypeptide chain conformation. The (*C'*-*exo*/*C'*-*endo*) ring pucker equilibria for the various turn structures are strongly influenced by stereoelectronic effects due to fluorine substitution and by steric interactions between the pyrrolidine ring substituents. The greatest energetic stabilization is observed under conditions in which the stereoelectronic interaction reinforces the preferred peptide chain conformation, i.e., the *C'*-*exo* pucker within type II β -turns of the model peptide (MeCO-4*R*-F-Pro-Gly-NHMe). Significant energetic destabilization occurs under conditions in which the stereoelectronically preferred ring pucker opposes the “preferred” peptide chain conformation, i.e., the *C'*-*endo* pucker within type II β -turns of the model peptide (MeCO-4*S*-F-Pro-Gly-NHMe). Similar results have been observed for 4-fluoroproline substitution in collagen-mimetic peptides in which structural stabilization was observed under conditions in which the ring pucker conformation of the fluoroproline epimer reinforced the local conformation of the polypeptide backbone of the collagen peptide in the triple helix structure.^{2–5}

Our results indicate that fluoroproline substitution may be employed as a mechanism to interrogate local conformational effects that arise due to the presence of proline residues in polypeptide sequences, particularly in situations in which preferences have been observed between particular ring pucker conformations and secondary structure elements.²⁵ This investigation suggests that turn structures may be included among local peptide structural elements that can be influenced through stereoelectronic control. As β -turn structures can exert a powerful influence to mediate protein folding events, stereoelectronic differences between proline analogues may be employed to address structural questions regarding the specific roles of proline-containing turn sequences in native protein conformations. For example, the “Pro-Gly” motif is a recurrent if not dominant structural feature associated with a number of native protein materials displaying elastomeric behavior.^{51–54} The molecular architectures of these protein-based elastomers differ from those of conventional synthetic elastomers, which suggests that different structural mechanisms may underlie their elastomeric behavior. Moreover, mechanical studies of the native

protein materials have indicated that the viscoelastic properties associated with the respective polypeptide sequences have been evolutionarily optimized for distinct biological function.⁵⁵ An understanding of the structural factors that determine the differences in mechanical behavior among native protein elastomers should provide criteria for the design of novel elastomeric materials in which the sequences can be tailored for specific technological applications. In addition, the mechanism of elasticity of elastin remains a subject of scientific disagreement, particularly as regards the origin of the elastomeric restoring force.^{56,57} The elastin structural variants reported in this study may be useful materials to discriminate between the relative contributions of main-chain versus solvation entropy to the elastomeric restoring force and provide information relevant to the debate over the mechanism of elasticity.

Experimental Section

Materials and Methods. Protein samples of **elastin-1**, **elastin-2**, and **elastin-3** were prepared via bacterial fermentation and purified via immobilized metal affinity chromatography as previously reported.¹⁸ The noncanonical amino acids (2*S*,4*S*)-4-fluoroproline and (2*S*,4*R*)-4-fluoroproline were purchased from Bachem Bioscience, Inc. (King of Prussia, PA). The ¹⁵N-labeled proteins were prepared from fermentations of *E. coli* expression strain DG99(*proC*::Tn10)/pAG2 in M9 minimal medium under supplementation with ¹⁵NH₄Cl (7.5 mM) and the appropriate proline derivative. The ¹⁵N labeled proteins were purified as described for unlabeled proteins. Protein solutions for analytical measurements were prepared from lyophilized specimens that were dissolved at the appropriate concentration in distilled, deionized water at 4 °C. Quantitative amino acid analysis was performed on aliquots of protein stock solutions (ca. 0.2–0.3 mg/mL) at the W. M. Keck Foundation Biotechnology Resource Laboratory of Yale University to provide accurate concentrations for CD spectroscopic experiments.

Physical and Analytical Measurements. The inverse temperature transitions of the elastin polypeptides were monitored as a function of temperature using an ultrasensitive differential scanning calorimeter (VP-DSC MicroCal, LLC, Northampton, MA). Protein samples were dissolved in distilled, deionized water at 4 °C in concentrations ranging from 0.5 to 2 mg/mL, degassed under dynamic vacuum and scanned from 5 to 60 °C at a rate of 60°/h. DSC data were processed using the program Origin (MicroCal, LLC, Northampton, MA), and T_i , ΔH , and ΔC_p values were calculated by curve fitting to the simplest appropriate model using the Levenberg-Marquardt nonlinear least-squares method.

Circular dichroism (CD) spectra were recorded on a Jasco J-810 spectropolarimeter equipped with a PFD-425S Peltier temperature control unit in 0.2 mm sealed quartz cells at concentrations of 5.8 μ M (**elastin-1**), 8.8 μ M (**elastin-2**), and 6.4 μ M (**elastin-3**) in distilled, deionized water. Temperature/wavelength CD-scans were performed within the temperature range from 5 °C to 65 °C with equilibration for 5 min at each temperature. The reversibility of the CD spectra was confirmed by scanning in the opposite direction of decreasing temperature with a similar equilibration period. Minimal hysteresis was observed between the forward and reverse scans under the conditions of polypeptide concentration employed in this study. Spectra were obtained from 260 to 190 nm at a resolution of 0.2 nm and at a scanning speed of 50 nm/min. The CD curves represented the average of five measurements and were smoothed using the means-movement method on the interval analysis of the spectral manager program. CD data are reported as mean residue ellipticity ($[\theta]$, deg cm² dmol⁻¹) in which

- (51) (a) Hayashi, C. Y.; Lewis, R. V. *J. Mol. Biol.* **1998**, *275*, 773–784. (b) Hayashi, C. Y.; Lewis, R. V. *Bioessays* **2001**, *23*, 750–756.
(52) Shewry, P. R.; Halford, N. G.; Belton, P. S.; Tatham, A. S. *Philos. Trans. R. Soc. London, Ser. B* **2002**, *357*, 133–142.
(53) Ardell, D. H.; Andersen, S. O. *Insect Biochem. Mol. Biol.* **2001**, *31*, 965–70.
(54) Cao, Q.; Wang, Y.; Bayley, H. *Curr. Biol.* **1997**, *7*, R677–R678.

- (55) Gosline, J.; Lillie, M.; Carrington, E.; Guerette, P.; Ortlepp, C.; Savage, K. *Philos. Trans. R. Soc. London, Ser. B* **2002**, *357*, 121–132.
(56) Li, B.; Alonso, D.; Bennion, B. J.; Daggett, V. *J. Am. Chem. Soc.* **2001**, *123*, 11991–11998.
(57) Urry, D. W.; Hugel, T.; Seitz, M.; Gaub, H. E.; Sheiba, L.; Dea, J.; Xu, J.; Parker, T. *Philos. Trans. R. Soc. London, Ser. B* **2002**, *357*, 169–184.

the molar masses of the polypeptides **elastin-2** and **elastin-3** were calculated on the basis of complete substitution of the canonical proline residues with the respective amino acid analogue.

NMR spectra were acquired on a Varian INOVA 600 (^1H , 599.74 MHz; ^{15}N , 60.78 MHz) at 4 °C. The NMR samples were prepared by dissolving the respective polypeptides in a $\text{H}_2\text{O}/\text{D}_2\text{O}$ (70:30) mixture at a concentration of 10 mg/mL. The pH of the specimens was adjusted to 2.7 to retard amide proton exchange on the NMR time scale. Chemical shifts for ^1H NMR spectra were referenced and reported relative to internal sodium 2,2-dimethyl-2-silapenta-5-sulfonate (0.0 ppm). Chemical shifts for ^{15}N NMR spectra were referenced and reported relative to 1 M urea (^{15}N , 98%+) in dimethyl sulfoxide as an external standard (77.0 ppm). Standard solvent suppression techniques were employed to reduce signal due to the residual protons of H_2O in the ^1H NMR of aqueous solutions of the polypeptides. Two-dimensional ^1H - ^1H NOESY NMR spectra were acquired in phase-sensitive mode using the hypercomplex method with a mixing time of 200 ms at a spectral width of 6799.8 Hz. Spectra were collected with 512 t_1 increments and 2048 complex data points with 32 scans. The ^1H - ^{15}N HSQC NMR spectra were acquired in phase-sensitive mode in which ^{15}N decoupling was applied for data acquisition. The spectral width was 6200.1 Hz for the ^1H channel and 2791.0 Hz for the ^{15}N channel. The data matrices contained 512 t_1 increments with 2048 complex points. The spectra were acquired with 32 scans per t_1 increment. The two-dimensional NMR data were further processed using the program NutsPro (Acorn NMR, Inc.).

Computational Methods. The second and third amino acids in the [Val-Pro-Gly-Val-Gly] moiety that serve as turn elements for the pentapeptide repeats were capped as follows: $\text{CH}_3\text{-C(=O)-Xaa-Gly-NH-CH}_3$ (**PG**). The latter was constructed in Macromodel⁵⁸ and conformationally manipulated to produce three reverse turns (β_1 , β_{II} , and inverse γ). Each turn type was modified to generate the corresponding C^γ -endo and C^γ -exo puckered proline conformers. The structures were further modified to add a fluorine atom at C-4 of the proline rings to produce the corresponding (4S)- and (4R)-fluoroproline-substituted structures. The corresponding 18 (**PG**) structures were optimized using the AMBER* force field to provide input to density functional theory (DFT) calculations. Several sets of optimizations and single-point calculations were performed on each structure as listed in Tables S1–S3 (cf. Supporting Information) employing the Gaussian-03 suite of programs.⁵⁹ The first phase of calculations optimized geometries using the Becke3LYP functional and the double- ζ 6-31G*

basis set (Beck3LYP/6-31G**/Beck3LYP/6-31G*). The second phase utilized the latter structures as input to a DFT triple- ζ (plus a diffuse function) optimization for the same set of structures (Beck3LYP/6311+G**/Beck3LYP/6-311+G*). The third phase employed (**PG**) geometries from both levels of calculation as input to a single-point energy evaluation using the more extensive triple- ζ Beck3LYP/6311+G(2d,p)//Beck3LYP/6-31G* and Beck3LYP/6311+G(2d,p)//Beck3LYP/6-311+G* basis sets. Finally, chemical shifts for ^{15}N in N–H of the central Gly engaged in the β -turn—corresponding to Gly³ of the VPGVG repeat unit—were estimated from the Gauge-Independent Atomic Orbital (GIAO) method as implemented in Gaussian-03 in combination with the MPW1PW91 and PBE protocols and calculated relative to an absolute shielding of 244.6 ppm for liquid ammonia at 25 °C.⁶⁰ The MPW1PW91 functional⁶¹ has been shown to provide reliable chemical shifts for ^{13}C , while the parameter-free PBE model⁶² proved superior for ^{15}N shifts in a six-way comparison. For the comparisons in Table 1, chemical shifts for ^{15}N in the Gly residue are expressed in ppm relative to 244.6 ppm. For example, for the fluorinated *exo*-F_{eq} type II β -turn, the Beck3LYP/6-311+G**/Beck3LYP/6-311+G* optimized structure delivers a raw isotropic chemical shift of 132.4 ppm. The NH_3 -adjusted relative shift was obtained from the equation $\delta(\text{endo-F}_{\text{eq}}) = \delta(\text{NH}_3) - \delta(\text{N-H}) = 244.6 - 132.4 = 112.2$ ppm. The corresponding isotropic PBE value of 121.4 ppm is then $\delta(\text{NH}_3) - \delta(\text{N-H}) = 244.6 - 121.4 = 123.2$ ppm.

Acknowledgment. The authors acknowledge the financial support of the Herman Frasch Foundation (418-97HF), NIH (5R01HL071136-04), and NSF (EEC-9731643). Studies at the NASA Ames Research Center were supported through the Center for Nanotechnology. W.K. and V.P.C. thank Dr. Shaoxiong Wu for assistance in acquisition of the NMR spectroscopic data. The CD spectropolarimeter was obtained from funds derived from an NSF grant (CHE-0131013).

Supporting Information Available: Two-dimensional ^1H - ^1H NOESY NMR spectroscopic assignments and a full tabular summary of the computational data for the polypeptides **elastin-1**, **elastin-2**, and **elastin-3**. This material is available free of charge via the Internet at <http://pubs.acs.org>.

JA054105J

(58) (a) Mohamadi, F.; Richards, N. G. J.; Guida, W. C.; Liscamp, R.; Lipton, M.; Caufield, C.; Chang, G.; Hendrickson, T.; Still, W. C. *J. Comput. Chem.* **1990**, *11*, 440–467. (b) <http://www.schrodinger.com/Products/macromodel.html>.

(59) Pople, J. A., et al. *Gaussian 03*, revision C.02; Gaussian, Inc.: Wallingford, CT, 2004.

(60) Brender, J. R.; Taylor, D. M.; Ramamoorthy, A. *J. Am. Chem. Soc.* **2001**, *123*, 914–922.

(61) (a) Adamo, C.; Barone, V. *J. Chem. Phys.* **1998**, *108*, 664–675. (b) Cimino, P.; Gomez-Paloma, L.; Duca, D.; Riccio, R.; Bifulco, G. *Magn. Reson. Chem.* **2004**, *42*, S26–S33.

(62) Adamo, C.; Barone, V. *Chem. Phys. Lett.* **1998**, *298*, 113–119.